RSC Advances

PAPER

View Article Online
View Journal | View Issue

Cite this: *RSC Adv.*, 2026, **16**, 2298

Efficient one-pot quinoline derivative synthesis from acetophenone and allyl alcohols

Fanjia Zeng,†[a] Yusheng Xu,†[a] Jiezhuang Fang,[a] Huawu Xu,[a] Yulin Cai,[a] Yixia Hong,[a] Junyan Gao,[a] Qinqiang Zeng*[b] and Xianzhe Su *[a]

Received 29th November 2025
Accepted 23rd December 2025

DOI: 10.1039/d5ra09229a

rsc.li/rsc-advances

Quinoline derivatives are widely found in pharmaceuticals, agrochemicals, and functional materials, and the development of efficient synthetic methods for these compounds has attracted considerable attention. In this study, we reported a strategy employing *O*-sulfonylhydroxylamine (HOSA) as a novel transient directing group (TDG) to achieve site-selective *ortho* C–H functionalization/cyclization of acetophenones with allyl alcohols. This reaction system operated under mild and readily tunable conditions, enabling efficient construction of the quinoline scaffold *via* a one-pot process. Our investigations revealed that the structure of the transient directing group, solvent, and reaction temperature collectively govern the reaction pathway, allowing precise control over product selectivity. This approach exhibited broad substrate scope and excellent functional group tolerance. This work not only represented the first application of HOSA as an efficient and versatile catalytic transient directing group in C–H cyclization reactions, but also provided a practical and valuable route for the synthesis of quinoline derivatives.

Introduction

Quinoline derivatives represent a privileged class of nitrogen-containing heterocyclic compounds extensively utilized in pharmaceuticals, agrochemicals, and functional materials due to their broad spectrum of biological activities.[1] They serve as key structural motifs in antimalarial drugs, anticancer agents, and antimicrobial compounds, while also finding applications as catalysts, solvents, and intermediates in organic synthesis.[2,3] Traditional synthetic approaches to quinolines, such as the Skraup and Doebner–Von Miller methods, often require strong acids, stoichiometric oxidants, and harsh reaction conditions, leading to limited functional group tolerance and environmental concerns.[4] Although the Friedländer synthesis offered improvement by condensing 2-aminobenzaldehydes with carbonyl compounds, it still depended on the availability of specifically functionalized aniline precursors.[5] These conventional methods typically involved multi-step procedures, poor atom economy, and difficulties in controlling regioselectivity, highlighting the need for more efficient and sustainable synthetic strategies.[6,7]

Transient directing groups (TDGs) have recently emerged as powerful tools for achieving site-selective C–H functionalization in transition metal catalysis. Unlike traditional directing groups that required installation and removal steps, TDGs reversibly formed imine or other dynamic covalent bonds with substrates, enabling temporary coordination to metals and facilitating proximal C–H activation without additional synthetic operations.[8,9] This strategy has been successfully implemented for functionalizing aldehydes and ketones, particularly in Pd(II)-catalyzed systems.[10] Notably, the group of Yu Jin-Quan[11] demonstrated the utility of glycine and related amines as catalytic TDGs for selective β-C(sp^3)–H arylation of ketones and aldehydes.[12] However, existing TDG approaches predominantly focused on simple functionalization reactions rather than complex annulations, and their application in constructing heterocyclic frameworks like quinolines remains largely unexplored.[12,13] Moreover, the ability to modulate reaction pathways through TDG design represented an ongoing challenge in C–H activation chemistry.[14] In numerous prior studies, it has been documented that aniline derivatives serve as starting materials and undergo cyclization with allyl alcohols in the presence of ruthenium-based catalysts (*e.g.*, $RuCl_2$(*p*-cymene)) to efficiently yield quinoline derivatives (Fig. 1a).[12,14]

In this study, we reported a novel one-pot synthesis of quinoline derivatives *via* transition metal-catalyzed pyridine cyclization between acetophenones and allyl alcohols, leveraging hydroxylamine-*O*-sulfonic acid (HOSA) as an efficient catalytic transient directing group (Fig. 1b). Our strategy enabled direct *ortho* C–H functionalization and subsequent cyclization of acetophenone derivatives without prefunctionalization, operating under mild conditions with excellent atom economy. The carefully designed TDG not only facilitated selective palladium-catalyzed C–H activation but also promoted the redox-neutral

[a]*Trauma Orthopedics Center, Shantou Hospital of Traditional Chinese Medicine, No. 3 Shaoshan Road, Shantou, Guangdong 515000, China. E-mail: STZYYYsu@163.com*
[b]*Shantou Hospital of Traditional Chinese Medicine, Shantou, Guangdong 515000, China. E-mail: 910617051@qq.com*
† Fanjia Zeng and Yusheng Xu contributed equally to this work.

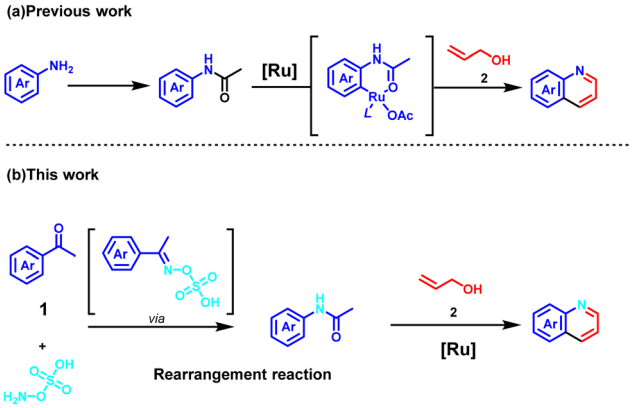

Fig. 1 The synthesis of quinoline derivatives in previous work (a) and this work (b).

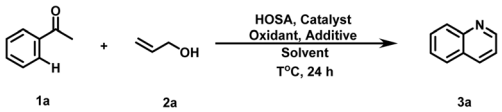

Fig. 2 The synthesis of product **3a**.

annulation with allyl alcohols through a sequence involving dehydrogenation, condensation, and cyclization. This method addressed several limitations of previous quinoline syntheses by offering exceptional functional group compatibility, broad substrate scope, and precise control over regioselectivity. Mechanistic studies revealed that the choice of TDG structure, solvent, and temperature critically influences the reaction pathway, allowing strategic diversion between different quinoline regioisomers. The development of this TDG-mediated annulation represented a significant advancement in sustainable heterocycle synthesis, providing a versatile and practical platform for accessing structurally diverse quinoline frameworks with potential biological applications.

Reaction condition optimization

Using acetophenone and allyl alcohol as the starting materials, and HOSA serving as both a TDG and a nitrogen source, we conducted reaction condition optimization studies by screening a series of reaction parameters including solvents, oxidants, and temperatures (see the SI for detailed reaction condition screening). Initial experiments employed a catalytic system consisting of the commercially available complex dichloro(pentamethylcyclopentadienyl)rhodium(III) dimer ($[Cp^*RhCl_2]_2$) and $AgSbF_6$. During the condition screening process, we observed a key phenomenon: in acetonitrile (MeCN) as the solvent, acetophenone could undergo a Beckmann rearrangement with HOSA to form acetanilide. Inspired by this observation, we attempted to subject the intermediate generated from the Beckmann rearrangement to a cyclization reaction with allyl alcohol for the synthesis of **3a** (Fig. 2).

Using a mixed solvent system of MeCN : HFIP = 1 : 2 (MeCN = acetonitrile; HFIP = hexafluoroisopropanol), a new pyridine ring was formed at 120 °C, and the yield of product **3a** was 30% (Table 1, entry 1). When the catalyst was replaced with $[RuCl_2(p\text{-cymene})]_2$, the yield of **3a** significantly increased (Table 1, entry 2). In contrast, when $[Cp^*IrCl_2]_2$, $[Cp^*RuCl_2]_2$, or Cp^*CoCOI_2 were used as catalysts, no reaction occurred, and the target product **3a** was not formed (Table 1, entries 3–5). When the oxidant was replaced with silver oxide (Ag_2O) or silver carbonate (Ag_2CO_3), either no reaction occurred or the yield was very low (Table 1, entries 6 and 7). When the mixed solvent system was replaced with MeCN : DMF = 1 : 2 (DMF = *N*,*N*-dimethylformamide) instead of MeCN : HFIP = 1 : 2, no reaction occurred (Table 1, entry 8). In comparison, using MeCN : MeOH = 1 : 2 (MeOH = methanol) as the mixed solvent system (replacing MeCN : HFIP = 1 : 2) promoted the formation of **3a** (Table 1, entry 9). Notably, when the mixed solvent system was switched to MeCN : DCE = 1 : 2 (DCE = 1,2-dichloroethane) instead of MeCN : HFIP = 1 : 2, the formation of **3a** was significantly improved, with a yield of 85% (Table 1, entry 10). To further enhance the yield, we screened the reaction

Table 1 Reaction condition optimization[a]

Entry	Catalyst	Oxidant	Solvent	*T* (°C)	Additive	Yield[b] (%)
1	$[Cp^*RhCl_2]_2$	$AgSbF_6$	MeCN : HFIP = 1 : 2	120 °C	$Cu(OAc)_2$	30
2	$[RuCl_2(p\text{-cymene})]_2$	$AgSbF_6$	MeCN : HFIP = 1 : 2	120 °C	$Cu(OAc)_2$	45
3	$[Cp^*IrCl_2]_2$	$AgSbF_6$	MeCN : HFIP = 1 : 2	120 °C	$Cu(OAc)_2$	NR
4	$[Cp^*RuCl_2]_2$	$AgSbF_6$	MeCN : HFIP = 1 : 2	120 °C	$Cu(OAc)_2$	NR
5	Cp^*CoCOI_2	$AgSbF_6$	MeCN : HFIP = 1 : 2	120 °C	$Cu(OAc)_2$	NR
6	$[RuCl_2(p\text{-cymene})]_2$	Ag_2O	MeCN : HFIP = 1 : 2	120 °C	$Cu(OAc)_2$	NR
7	$[RuCl_2(p\text{-cymene})]_2$	Ag_2CO_3	MeCN : HFIP = 1 : 2	120 °C	$Cu(OAc)_2$	26
8	$[RuCl_2(p\text{-cymene})]_2$	$AgSbF_6$	MeCN : DMF = 1 : 2	120 °C	$Cu(OAc)_2$	NR
9	$[RuCl_2(p\text{-cymene})]_2$	$AgSbF_6$	MeCN : MeOH = 1 : 2	120 °C	$Cu(OAc)_2$	48
10	$[RuCl_2(p\text{-cymene})]_2$	$AgSbF_6$	**MeCN : DCE = 1 : 2**	**120 °C**	$Cu(OAc)_2$	**85**
11	$[RuCl_2(p\text{-cymene})]_2$	$AgSbF_6$	MeCN : DCE = 1 : 2	100 °C	$Cu(OAc)_2$	36
12	$[RuCl_2(p\text{-cymene})]_2$	$AgSbF_6$	MeCN : DCE = 1 : 2	110 °C	$Cu(OAc)_2$	77
13	$[RuCl_2(p\text{-cymene})]_2$	$AgSbF_6$	MeCN : DCE = 1 : 2	130 °C	$Cu(OAc)_2$	83
14	$[RuCl_2(p\text{-cymene})]_2$	$AgSbF_6$	MeCN : DCE = 1 : 2	120 °C	AcOH	30
15	$[RuCl_2(p\text{-cymene})]_2$	$AgSbF_6$	MeCN : DCE = 1 : 2	120 °C	NaOAc	45
16	$[RuCl_2(p\text{-cymene})]_2$	$AgSbF_6$	MeCN : DCE = 1 : 2	120 °C	CsOAc	50

[a] Reaction conditions:**1** (0.5 mmol), **2** (0.75 mmol), HOSA (1.0 mmol), catalyst (5.0 mol%), oxidant (1.0 mmol), additive (2 mmol), in the solvent (3.0 mL) for 24 h. [b] Yields of isolated products.

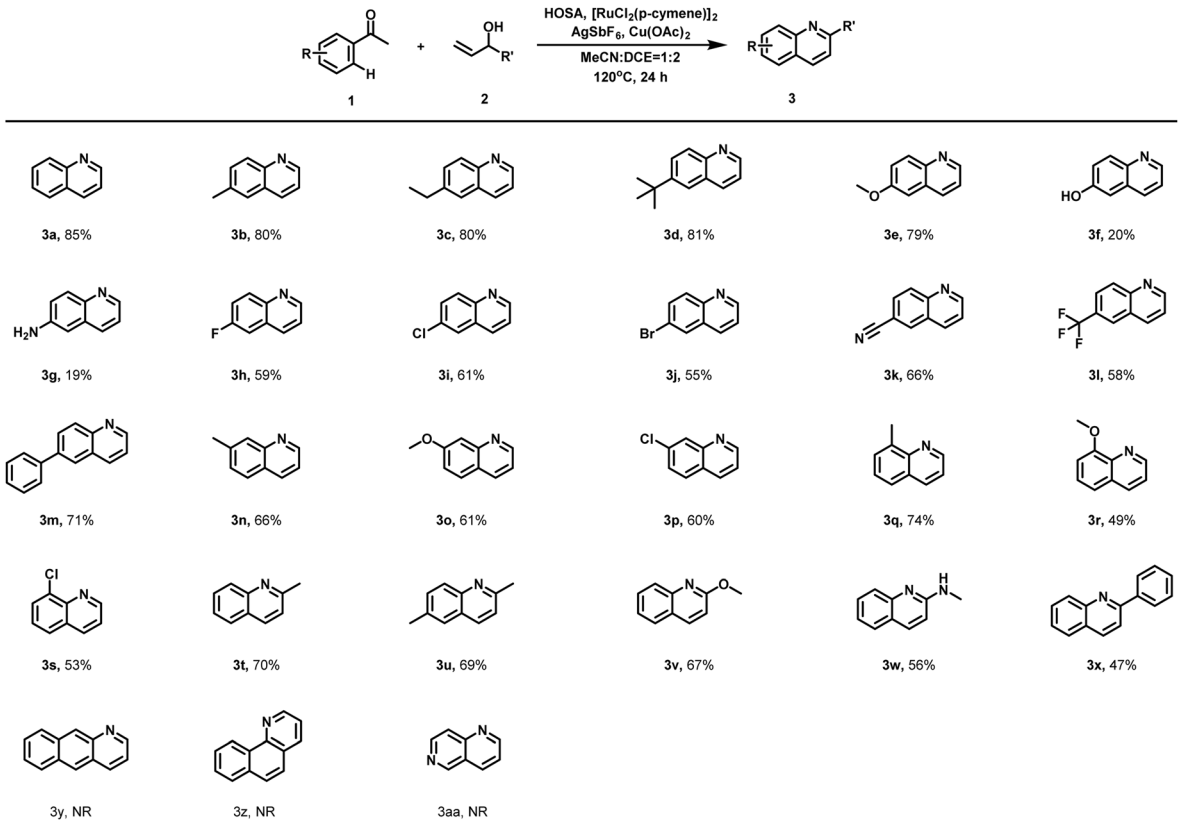

Fig. 3 Synthesis of product **3**.[a] [a]Reaction conditions: **1** (0.5 mmol), **2** (0.75 mmol), HOSA (1.0 mmol), $[RuCl_2(p\text{-cymene})]_2$(5.0 mol%), $AgSbF_6$ (1.0 mmol), $Cu(OAc)_2$(2 mmol), in the solvent (MeCN : DCE = 1 : 2) (3.0 mL) for 24 h. [b]Yields of isolated products.

temperature and found that both decreasing and increasing the temperature led to a reduction in yield (Table 1, entries 11–13), indicating that 120 °C might be the optimal reaction temperature. Finally, when the additive was replaced with AcOH (acetic acid), NaOAc (sodium acetate), or CsOAc (cesium acetate), the yields were all lower than that achieved with $Cu(OAc)_2$ (copper(II) acetate) (Table 1, entries 14–16).

To evaluate the generality of the developed protocol, we investigated the substrate scope by varying substituents on acetophenone derivatives and allyl alcohols. The results were summarized for products **3a–3x**, **3aa**, **3y**, and **3z** as depicted (Fig. 3). All yields reported were those of isolated products, and the reaction conditions were as follows: **1** (0.5 mmol), **2** (0.75 mmol), $[RuCl_2(p\text{-cymene})]_2$ (5.0 mol%), $AgSbF_6$ (1.0 mmol), $Cu(OAc)_2$ (2 mmol), in MeCN : DCE (1 : 2, 3.0 mL) at 120 °C for 24 h. Acetophenones bearing *para*-electron-donating groups underwent the reaction smoothly. *para*-Methyl substituted acetophenone afforded **3b** in 80% yield, *para*-ethylacetophenone afforded product **3c** in 80% yield, while *para-tert*-butylacetophenone gave product **3d** in 81% yield. While *para*-methoxy substituted acetophenone gave **3e** in 79% yield. *para*-Phenyl substituted acetophenone yielded **3m** in 71% yield. Notably, *para*-methyl substituents at different positions on the quinoline framework were well-tolerated, as seen in **3n** (66% yield, methyl on the phenyl ring) and **3t** (70% yield, methyl on the quinoline ring). For *para*-electron-withdrawing groups, the protocol exhibited good compatibility. *para*-Fluoro (**3h**, 59%), *para*-chloro (**3i**, 61%), *para*-bromo (**3j**, 55%), *para*-cyano (**3k**, 66%), and *para*-trifluoromethyl (**3l**, 58%) substituted acetophenones all furnished the corresponding quinoline products. *para*-Amino substituted acetophenone gave **3g** in 19% yield, likely due to competitive coordination of the amino group. *meta*-Substituted acetophenones were also viable substrates. *meta*-Methoxy substituted acetophenone afforded **3o** in 61% yield, and *meta*-chloro substituted acetophenone gave **3p** in 60% yield, indicating that *meta* substituents did not significantly impede the reaction. *ortho*-Substituted acetophenones were tested as well. *ortho*-Methyl substituted acetophenone produced **3q** in 74% yield, *ortho*-methoxy substituted acetophenone gave **3r** in 49% yield, and *ortho*-chloro substituted acetophenone afforded **3s** in 53% yield. *ortho*-Substituents on the acetophenone were also tolerated: **3u** (69%, *ortho*-methyl) and **3v** (67%, *ortho*-methoxy) were isolated in moderate to good yields. Additionally, *ortho*-amino (**3w**, 58%) and *ortho*-phenyl (**3x**, 47%) substituted quinoline derivatives were obtained. Allyl alcohols with different R′ substituents were investigated. Propyl-substituted allyl alcohol gave **3c** in 80% yield, and *tert*-butyl substituted allyl alcohol afforded **3d** in 81% yield. Hydroxyl-substituted quinoline **3f** was obtained in 20% yield, presumably due to the sensitivity of the hydroxyl group under the reaction conditions. We also explored other aryl ethyl ketones and challenging substrates. However, 1-naphthyl ethyl

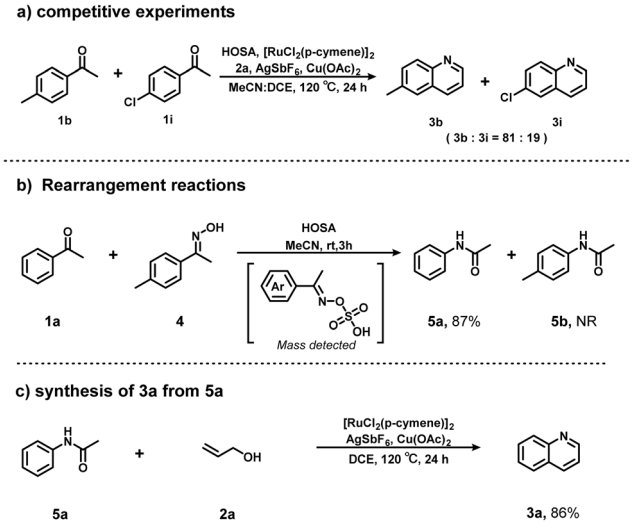

Fig. 4 Mechanistic studies. Reaction conditions: (a) **1b** (67.1 mg), HOSA (113.1 mg), **1i** (77.3 mg), $[RuCl_2(p\text{-cymene})]_2$ (5.0 mol%), $AgSbF_6$ (1.0 mmol), $Cu(OAc)_2$ (2 mmol), in the solvent (MeCN : DCE = 1 : 2) (3.0 mL) for 24 h. (b) **1a** (60.1 mg), **4** (74.6 mg), HOSA (113.1 mg), in the MeCN for 3 h. (c) **5a** (0.5 mmol, 1.0 equiv.), **2a** (43.6 mg), $[RuCl_2(p\text{-cymene})]_2$ (0.025 mmol, 5 mol%), $AgSbF_6$ (0.25 mmol, 0.5 equiv.), $Cu(OAc)_2$ (1.0 mmol, 2.0 equiv.) and in the DCE for 24 h. [b]Yields of isolated products.

ketone (**3y**), phenanthrenyl ethyl ketone (**3z**), and pyridyl ethyl ketone (**3aa**) resulted in no reaction (NR), highlighting the limitations of the protocol toward these polycyclic or heterocyclic aryl ketones.

Mechanistic studies

To elucidate the reaction mechanism, we performed competition experiments to verify the effect of electronic properties on the cyclization reaction. It was found that the yield of *para*-methyl acetophenone **1b** (electron-donating) was higher than that of *para*-chloro acetophenone **1i** (electron-withdrawing) (Fig. 4a). The conditions for the Beckmann rearrangement and the advantages of our developed method were illustrated in Fig. 4b. Specifically, acetophenone (**1a**), (*E*)-1-(*p*-tolyl)ethan-1-one oxime (**4**), and HOSA were reacted in acetonitrile as the solvent, affording **5a** in a high yield of 87% without the formation of **5b**, indicating that HOSA could promote the intramolecular Beckmann rearrangement. Subsequently, under Ru(II) catalysis, **5a** reacted with **2a** in the absence of HOSA to afford the target product **3a** in a high yield (Fig. 4c), indicating that the reaction involved a Ru(II)-catalyzed C–H activation process and also confirming the effectiveness of HOSA-mediated conversion of ketone to amide.

The proposed mechanism for the formation of product **3a** involved the following sequence of steps[5] (Fig. 5): acetophenone (**1a**) first reacted with HOSA to generate intermediate **IN1**. **IN1** then underwent an intramolecular Beckmann rearrangement, facilitated by HOSA, to form **IN2**. In the presence of $Cu(OAc)_2$, the dimer $[RuCl_2(p\text{-cymene})]_2$ dissociated to generate the active species $Ru(p\text{-cymene})(OAc)_2$. This active species bound to **IN2** *via* *O*-coordination, followed by *O*-metallation and subsequent *ortho* C–H activation, leading to the formation of a six-membered ruthenacycle **IN3**. Meanwhile, **2a** was oxidized by $Cu(OAc)_2$ to form propenone **IN4**. **IN3** underwent olefin coordination with **IN4** to produce **IN5**, which then underwent double bond insertion to form a six-membered ruthenacycle **IN6**. **IN6** underwent β-hydride elimination and reductive elimination to yield the final product **3a**. Simultaneously, $AgSbF_6$ reoxidized the Ru(*p*-cymene) species back to $Ru(p\text{-cymene})(OAc)_2$, thus sustaining the catalytic cycle.

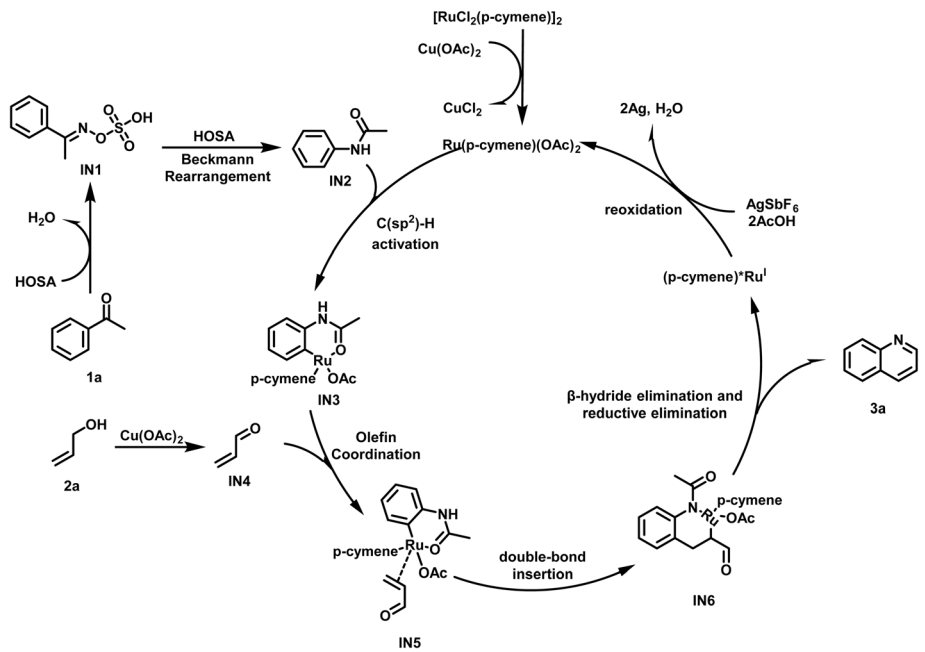

Fig. 5 Proposed mechanism.

Conclusion

In summary, we have successfully developed an efficient one-pot pyridine cyclization strategy for the synthesis of quinoline derivatives *via* the reaction of acetophenones with allyl alcohols, leveraging *O*-sulfonylhydroxylamine (HOSA) as a novel catalytic transient directing group (TDG). This work represented the first application of HOSA as a versatile and efficient TDG in C–H activation/cyclization reactions, addressing the long-standing need for practical methods to construct quinoline scaffolds. The developed protocol exhibited notable advantages: it operated under mild and readily tunable reaction conditions, eliminated the requirement for prefunctionalized substrates, and demonstrated broad substrate scope with excellent functional group tolerance—features that are particularly valuable for accessing structurally diverse quinoline derivatives relevant to pharmaceuticals, agrochemicals, and functional materials. Mechanistic and condition-optimization studies further revealed that the structure of HOSA (as TDG), solvent selection, and reaction temperature collectively govern the reaction pathway, enabling precise control over product selectivity and ensuring efficient formation of the target quinoline products (Fig. 5). Beyond providing a practical route for quinoline synthesis, this study also expanded the toolkit of transient directing groups for C–H functionalization, offering new insights into the design of TDG-mediated cyclization reactions. We anticipate that this strategy will serve as a valuable platform for the synthesis of other nitrogen-containing heterocycles and inspire further developments in sustainable and site-selective C–H activation chemistry.

Author contributions

Fanjia Zeng: writing, review and editing, methodology, conceptualization. Yusheng Xu: writing, review and editing, methodology, conceptualization. Jiezhuang Fang: visualization, data curation. Huawu Xu: visualization, data curation. Yulin Cai: formal analysis. Yixia Hong: validation. Junyan Gao: validation. Qinqiang Zeng: supervision, review and editing. Xianzhe Su: supervision, review and editing.

Conflicts of interest

There are no conflicts to declare.

Data availability

The data supporting this article have been included as a part of the supplementary information (SI). Reagents and protocols are available from the corresponding author upon reasonable request. Supplementary information is available. See DOI: https://doi.org/10.1039/d5ra09229a.

Acknowledgements

This work was supported by the Medical and Health Category of Shantou Science and Technology Plan (No. 190821215263629).

References

1 N. Goswami, T. Bhattacharya and D. Maiti, Transient Directing Ligands for Selective Metal-Catalysed C–H Activation, *Nat. Rev. Chem.*, 2021, **5**, 646–662.
2 A. V. Muller, S. P. Desai, C. Cappuccino, C. L. Donley, A. J. M. Miller, J. M. Mayer, D. C. Grills, D. E. Polyansky and J. J. Concepcion, Regeneration of Benzimidazole-Based Organohydrides Mediated by Ru Catalysts, *ACS Catal.*, 2025, **15**, 14996–15008.
3 Z. Ren, X. Si, J. Chen, X. Li and F. Lu, Catalytic Complete Cleavage of C–O and C–C Bonds in Biomass to Natural Gas over Ru(0), *ACS Catal.*, 2022, **12**, 5549–5558.
4 P. B. Staub, H. M. Holst, N. N. Puthalath and C. J. Douglas, Chiral Transient Directing Groups for Catalytic Asymmetric Intramolecular Alkene Hydroacylation, *ACS Catal.*, 2025, **15**, 11512–11518.
5 G. S. Kumar, P. Kumar and M. Kapur, Traceless Directing-Group Strategy in the Ru-Catalyzed, Formal [3 + 3] Annulation of Anilines with Allyl Alcohols: A One-Pot, Domino Approach for the Synthesis of Quinolines, *Org. Lett.*, 2017, **19**, 2494–2497.
6 N. Sabat, L. P. Slavetínska, B. Klepetarova and M. Hocek, C–H Imidation of 7-Deazapurines, *ACS Omega*, 2018, **3**, 4674–4678.
7 K. Ghosh, Y. Nishii and M. Miura, Oxidative C–H/C–H Annulation of Imidazopyridines and Indazoles through Rhodium-Catalyzed Vinylene Transfer, *Org. Lett.*, 2020, **22**, 3547–3550.
8 L. Zhang, L.-L. Wang and D.-C. Fang, DFT Case Study on the Comparison of Ruthenium-Catalyzed C–H Allylation, C–H Alkenylation, and Hydroarylation, *ACS Omega*, 2022, **7**, 6133–6141.
9 I. Beckers, B. Krasniqi, P. Kumar, D. Escudero and D. De Vos, Ligand-Controlled Selectivity in the Pd-Catalyzed C–H/C–H Cross-Coupling of Indoles with Molecular Oxygen, *ACS Catal.*, 2021, **11**, 2435–2444.
10 V. K. Maikhuri, M. Rawat and D. S. Rawat, Recent Advances in the 3d-Transition-Metal-Catalyzed Synthesis of Isoquinolines and Its Derivatives, *Adv. Synth. Catal.*, 2023, **365**, 4458–4494.
11 F.-L. Zhang, K. Hong, T.-J. Li, H. Park and J.-Q. Yu, Functionalization of C(sp^3)-H bonds using a transient directing group, *Science*, 2016, **351**, 252–256.
12 K. Yokoo and K. Mori, Expeditious Synthesis of Multisubstituted Quinolinone Derivatives Based on Ring Recombination Strategy, *Org. Lett.*, 2020, **22**, 244–248.
13 S. Kirad, P. R. Deepa and M. Sankaranarayanan, Greener Alternatives for Synthesis of Isoquinoline and Its Derivatives: A Comparative Review of Ecocompatible Synthetic Routes, *RSC Adv.*, 2025, **15**, 30231–30275.
14 Q.-Z. Zheng and N. Jiao, Ag-Catalyzed C–H/C–C Bond Functionalization, *Chem. Soc. Rev.*, 2016, **45**, 4590–4627.